Computer Modeled Multiportal Approaches to the Skull Base

Randall A. Bly[1] David Su[2] Blake Hannaford[3] Manuel Ferreira Jr.[2] Kris S. Moe[1]

[1] Department of Otolaryngology–Head and Neck Surgery, University of Washington School of Medicine, Seattle, Washington, United States
[2] Department of Neurological Surgery, University of Washington School of Medicine, Harborview Medical Center, Seattle, Washington, United States
[3] Department of Electrical Engineering, University of Washington, BioRobotics Laboratory, Office of Sponsored Programs, Seattle, Washington, United States

Address for correspondence and reprint requests Kris S. Moe, MD, Department of Otolaryngology–Head and Neck Surgery, University of Washington School of Medicine, 1959 NE Pacific Street, Box 356515, NE-306, Seattle, WA 98195-6515, United States (e-mail: krismoe@uw.edu).

J Neurol Surg B 2012;73:415–423.

Abstract

Skull base surgical approaches have evolved significantly to minimize collateral tissue damage and improve access to complex anatomic regions. Many endoscopic surgical portals have been described, and these can be combined in multiportal approaches that permit improved angles for visualization and instrumentation. To assist in the choice of entry portal and surgical pathway analysis, a three-dimensional computer model with virtual endoscopy was created. The model was evaluated on transnasal and transorbital approaches to access 11 specified sellar and parasellar target locations on 14 computed tomography (CT) scans. Data were collected on length of approach, angle between instruments, and approach angle with respect to anatomical planes. Optimal multiportal approach combinations were derived. The data demonstrated that the shortest, most direct pathway to many sellar and parasellar targets was through transorbital portals. Distances were reduced by 35% for certain target locations; combining transorbital and transnasal portals increased the angle between instruments 4-fold for many targets. The predicted values from the model were validated on four cadaver specimens. Computer modeling holds the potential to play an integral role in the design, analysis, and testing of new surgical approaches, as well as in the selection of optimal approach strategies for the unique pathology of individual patients.

Keywords
- computer model
- pituitary
- sella
- anterior skull base
- approach planning
- virtual endoscopy
- multiportal

Introduction

Skull base surgery has evolved rapidly over the past two decades, utilizing advances in optics, materials, instrumentation, and surgical navigation. This has been particularly apparent in pituitary surgery. Skull base centers have demonstrated impressive endoscopic transnasal access to regions around the pituitary, such as Meckel's cave.[1] Transnasal endoscopic approaches continue to develop and improve access to new anatomical locations, and new approach portals are being developed that also provide excellent visualization and access to skull base targets.

Access to a target is not the sole determinant of a successful surgical outcome. Intrinsic characteristics of the pathology, such as tumor aggressiveness and physical consistency, are all critical parameters.[2] Multiportal endoscopic techniques offer the ability to approach, visualize, and manipulate pathology from various perspectives, which could lead to improved surgical outcomes.

The goal of multiportal approaches is to improve the surgeon's ability to access, visualize, and manipulate a

received
February 28, 2012
accepted after revision
August 13, 2012
published online
November 16, 2012

DOI http://dx.doi.org/10.1055/s-0032-1329623.
ISSN 2193-6331.

surgical target while minimizing collateral damage. There are two main types of collateral damage: pathway trauma or target trauma. Pathway trauma refers to the damage incurred by the dissection to reach the target, including injuries associated with retraction and repetitive passage of instruments. Target trauma refers to damage to healthy adjacent tissue when manipulating the target pathology. Target trauma may be reduced by enhanced visualization and microsurgical dissection, but the degree of injury is largely dictated by the type of pathology. Pathway trauma, however, can be minimized by appropriate choice of surgical portals and pathways. Thus, to decrease collateral tissue damage, an emphasis should be placed on optimizing the selection of approach portal combinations that provide optimal visualization with the least possible tissue dissection and damage.

Many portals to access the skull base and brain have been described in addition to the transnasal approach. These include transoral, transorbital, supraorbital, transcervical, transhyoid, transmaxillary, and transventricular. Case reports of transnasal and transventricular combined approaches to remove large pituitary adenomas are examples of successful multiportal interventions that minimize collateral injury to healthy tissue.[3–6] For other tumor locations in the skull base, the optimal choice of a surgical portal may not be intuitive; an approach may allow access to the desired location but may not be ideal in avoidance of critical neurovascular structures, dissection capability, visualization, or the angle of target manipulation. A method for evaluating and planning these multiportal approaches is needed.

The utility of analyzing endonasal approaches with a three-dimensional computer model has been demonstrated in recent publications. A model was created for teaching purposes, surgical planning, and to determine the extent of bone removal required in the approach.[7,8] Other researchers have created models to teach complex anatomy, such as that encountered in a transpetrosal surgical approach.[9,10] Simulators for sinus surgery have been developed with integrated haptic feedback for teaching purposes.[11] A radioanatomic study has quantified approach angles to determine the extent of maxillectomy necessary to reach locations in the infratemporal fossa.[12] Patient-specific virtual visualization for presurgical rehearsal and planning has been found to be helpful in the resection of cerebral gliomas.[13] Other methods to quantify approaches have included the development of a scoring system that grades the quality of an approach in cadaver anatomical studies.[14]

A model offers the potential to solve problems in a systematic way by considering access to a specific region in the skull base as a complex three-dimensional problem that has variables and constraints. In theory, an optimal surgical approach exists that is a function of target location, anatomy, and surgical portals. Our goal is to create an algorithm within the model that solves this complex problem to optimize visualization and the ability to perform surgical tasks at the target location. The result may be a new approach or approach combination, and a computer model is a logical environment to first perform analyses and feasibility tests.

With hundreds of potential skull base targets and over 20 surgical portals described to date, there are thousands of possible approach combinations that must be considered in the model. To simplify for this initial analysis, one region was chosen and the number of portals was limited. Regions adjacent to the sella were chosen because they are locations that frequently require surgical access. Although transnasal approaches are most commonly used for this region, prior studies have demonstrated an improved working area in this region utilizing a supraorbital portal.[15,16] Transorbital approaches follow the contour of the bony orbit and offer safe approaches to these regions while also providing a wide range of approach angles.[17–19] The surgical portals chosen for inclusion in the model in this study were two transnasal and eight transorbital (four around each orbit).

Methods

A computer model was created using iNtellect Cranial Navigation (Version 1.1–14, Stryker Corporation, Kalamazoo, MI, USA) software that generates a three-dimensional coordinate system, good spatial visualization, and the ability to show approach vectors, define volumes, and perform virtual endoscopy. Fourteen CT scans of normal skull base anatomy (eight males and six females, age range 23 to 65) were used to generate normative data. The pituitary gland, internal carotid arteries, cavernous sinuses, and optic nerves and chiasm were defined as three-dimensional volumes in the model. Eleven specific locations of the sella and parasellar regions were evaluated and labeled for visualization (►**Table 1**). These were chosen as locations that complex pituitary lesions may extend into, and an optimized multiportal approach could be defined for each.

The 10 possible surgical portals (two nasal and eight transorbital) were defined at their entry point at the skin or nasal vestibule. The transnasal entry points were defined as lateral as possible at the nasal vestibule, limited laterally by the pyriform aperture in the approach vector. The transorbital portal entry points were placed at the four quadrants, previously described as precaruncular (medial), superior lid crease (superior), lateral retrocanthal (lateral), and preseptal (inferior).[17] The 10 entry portals were systematically visualized for each target location. Combinations were limited to one approach per orbit so that retraction on the globe was due to only one portal. The combinations were assessed for gross feasibility. Virtual endoscopy was performed through each portal, visualizing the target location and the vectors of approach as instruments reached the target from the other portals in that combination. Approach combinations for each target location were derived using the criteria listed in ►**Table 2**.

Of the feasible combinations, the (x, y, z) coordinates were recorded for each portal entry point and the target location point. The process was then repeated for all 11 target locations. Midsagittal and skull base planes were defined by choosing points in the midline at the crista galli and posterior internal occipital protuberance, and between the posterior clinoid processes as well as the tuberculum sellae,

Table 1 Target locations and surgical portals

Target locations	Surgical portals
1. Prechiasmatic	1. Right transnasal
2. Postchiasmatic	2. Left transnasal
3. Right cavernous sinus	3. Right superior lid crease (superior orbit wall)
4. Left cavernous sinus	4. Right lateral retrocanthal (lateral orbital wall)
5. Right Meckel's cave	5. Right transconjunctival (inferior orbital wall)
6. Left Meckel's cave	6. Right precaruncular (medial orbital wall)
7. Right superior orbital fissure	7. Left superior lid crease (superior orbit wall)
8. Left superior orbital fissure	8. Left lateral retrocanthal (lateral orbital wall)
9. Third ventricle extension	9. Left transconjunctival (inferior orbital wall)
10. Basal cistern extension	10. Left precaruncular (medial orbital wall)
11. Clivus	–

respectively. These points were used to define the coordinate system with respect to sagittal and skull base anatomic planes. This later permitted approach angle calculations with respect to these planes. ►**Fig. 1** shows all 10 entry portals with approach vectors to the prechiasmatic location.

For each CT scan, there were 11 targeted locations, 10 entry portal locations, 4 points to define anatomic planes totaling 25 (x, y, z) data points. ►**Fig. 2** shows the software interface where the data points were chosen and exported. In addition, for each target location, the optimal multiportal combinations were recorded that satisfied the criteria in ►**Table 2**. This data was then processed with a Matlab (MathWorks, Natick, Massachusetts, USA) code written to compute the angle between vectors that defined the approach portal trajectories, the angle of the approach vector with respect to the defined anatomic planes, and the distances from the portal entry points to the target. The angles were calculated using the linear algebraic relationship between two vectors (A and B) in three-dimensional space and the angle between them (θ): $\cos(\theta) = A \cdot B / \|A\| \cdot \|B\|$. Where $A \cdot B$ is the scalar product (dot product) of vectors A and B, and $\|A\|$ denotes the magnitude of vector A.

Table 2 Criteria used to choose surgical approach combinations in the model

1.	The approach is feasible based on virtual endoscopy and three-dimensional visualization
2.	No vital neurovascular structures are traversed
3.	The angle between instruments is >15 degrees (the approximate angulation between two transnasal instruments)
4.	The new approach combination provides an approach angle with respect to a skull base plane or sagittal plane that is >15 degrees different than standard transnasal approaches
5.	The distance to the target is reduced significantly compared with transnasal approaches
6.	Only one approach per orbit may be included in the combination

A cadaver study was performed to test the approach configurations determined to be optimal with the computer model. CT scans were performed on four cadaver head specimens, and surgical navigation was used. These four CT scans were included in the above computer model data collection. The multiportal approaches to reach each target were demonstrated. While performing the operations on the cadaver specimens, distances to target locations were measured as well as intra-instrument distance, which was used to calculate the angle between instruments using the law of cosines. ►**Figs. 3** and **4** are photographs demonstrating combinations of endoscope and instruments through various approach portals in a cadaver specimen.

Results

The analysis of 10 approaches to the 11 targets yielded over 100 distances and 1000 unique angle results. When evaluating the approach to a particular target, the number of portals possible was reduced to those deemed potentially feasible. Virtual endoscopy provided qualitative evaluation of approaches prior to being performed on a cadaver specimen. Only the approaches that satisfied the criteria in ►**Table 2** were further analyzed on a cadaver specimen. Virtual endoscopy could be performed through any portal to access any target location, and it also permitted the visualization of vital structures incorporated into the model as well as the trajectory of instruments from other portals (►**Fig. 5**).

In the case of the left cavernous sinus as a target location, the portals that were selected for further analysis included bilateral transnasal, medial orbit, superior orbit, and lateral orbit portals. ►**Fig. 6** shows the angles between instruments that are possible for the cavernous sinus target location. These ranged from 13.9 degrees in the case of the bilateral nasal portals to 58.7 degrees when utilizing a combination of medial and lateral orbit portals. Examining the approach angle created against a midsagittal plane, the range was

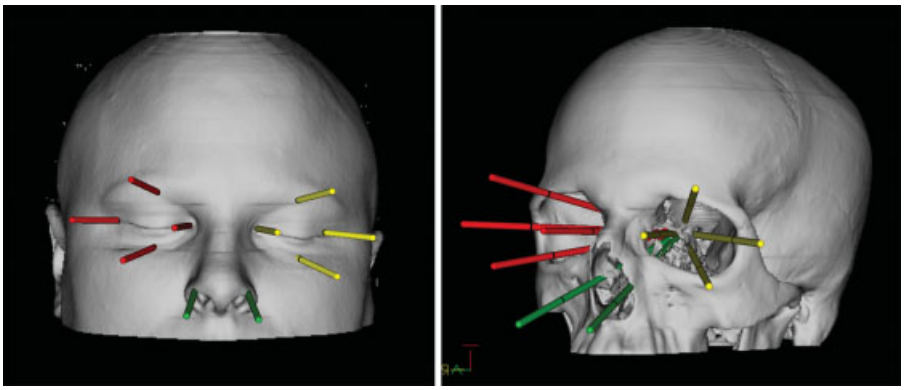

Fig. 1 The 10 possible entry points with approach vectors to a prechiasmatic target.

about 60 degrees. The ipsilateral lateral orbit portal had an approach angle of 35.1 degrees on one side of the midsagittal plane, and the contralateral nasal and medial orbit portals permitted a 16.7 and 25.0 (denoted as negative values in ►**Fig. 7b**) degree approach from the other side of the plane, respectively. This is visualized in ►**Fig. 7b** in the axial plane view. The distance measurements ranged from 99.5 mm for the contralateral nasal portal to 64.3 mm for the ipsilateral medial orbit portal.

The approach to Meckel's cave had the greatest number of possible approaches. Similar ranges in angles that were seen for the cavernous sinus target were also found for the Meckel's cave and superior optic fissure targets, 14.0 to 60.0 degrees and 16.2 to 76.1 degrees, respectively. The symmetric approach combinations were averaged for each target location, which incorporated anatomical information from 28 orbits from the 14 CT scans that were analyzed. For example, the calculations from a left nasal and right medial orbit

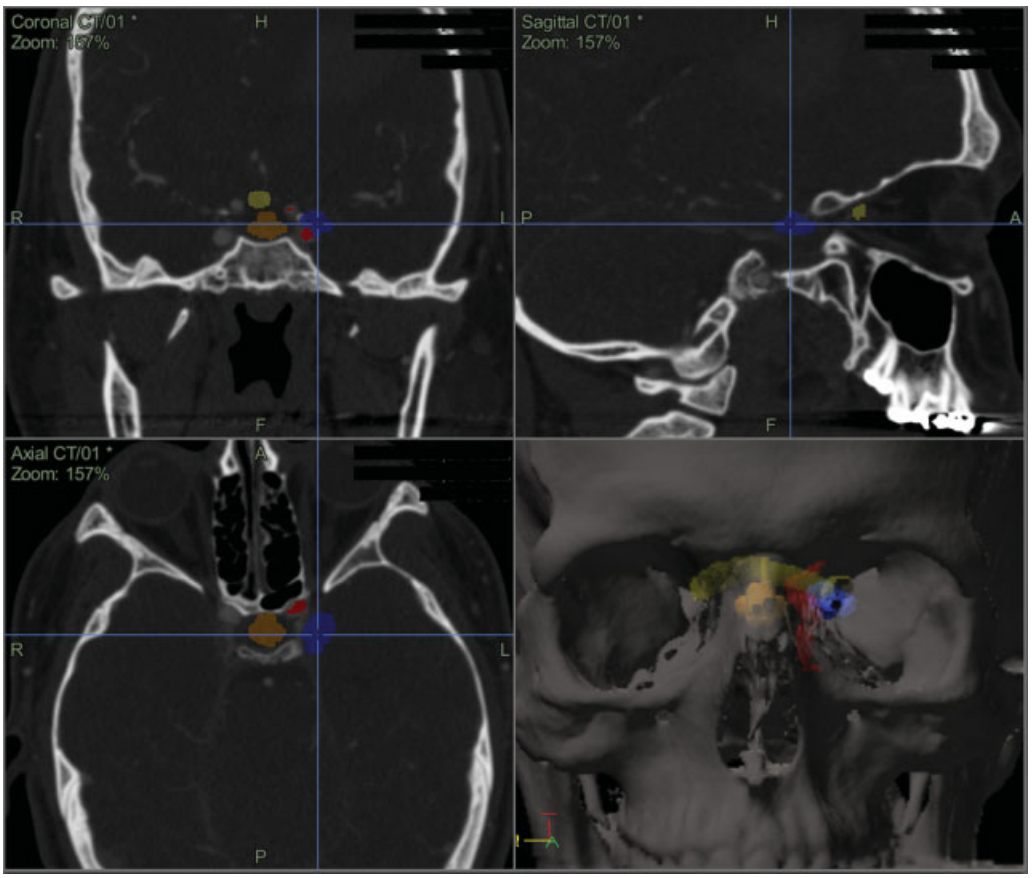

Fig. 2 Software interface with volumes defined for the carotid artery, cavernous sinus, pituitary, and optic nerve segment. The cursor has selected a point within the left cavernous sinus in this instance. Volumes defined for optic nerve and chiasm (yellow), internal carotid artery (red), cavernous sinus (blue), and pituitary gland (beige) are depicted.

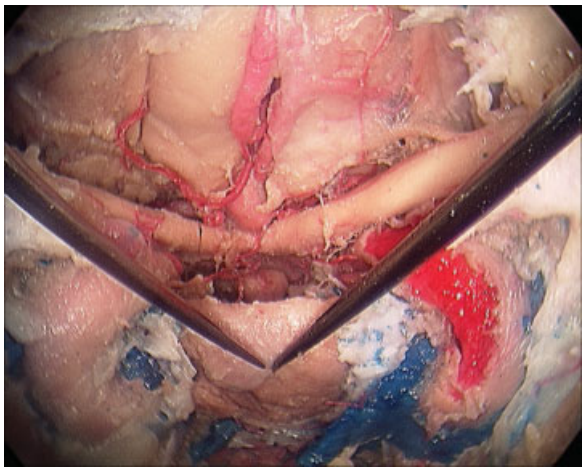

Fig. 3 Endonasal view of instruments from bilateral medial orbit portals approaching the pituitary gland.

Fig. 4 Endoscopic view through the right medial orbit portal with instruments from left medial orbit and left nasal portals approaching the pituitary gland.

combination to reach a left-sided target were averaged with the right nasal and left medial orbit combinations to reach a right-sided target.

The skull base plane was defined by the intersection of the tuberculum sellae and posterior clinoid processes. The approach angle with respect to this plane varied similarly for the three nonmidline targets and had a total range of approximately 33 degrees. In the case of the cavernous sinus target, nasal portals approached the plane from 17.2 degrees below (denoted as a negative number in ►**Fig. 7c**), medial orbit portals approached the plane from 4.6 degrees above (denoted positive), and superior orbit portals approached the plane from 15.7 degrees above.

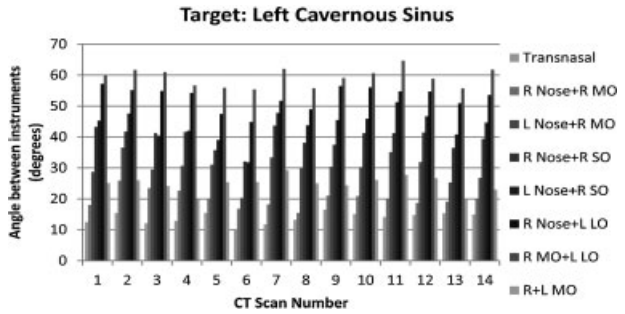

Fig. 6 Angles between instruments for varying portal combinations for the left cavernous sinus target location. CT, computed tomography; L, left; LO, lateral orbit; MO, medial orbit; R, right; SO, superior orbit.

The symmetric approaches for midline target locations (pre and postchiasmatic, third ventricle, basal cistern, and clivus) were averaged, incorporating anatomical information from 28 orbits on the 14 CT scans analyzed. For example, the right nasal and left medial orbit portals were averaged with the left nasal and right medial orbit portals for a given target. Angles between instruments varied from 14.7 degrees with bilateral nasal portals to 41.9 degrees with a nasal and superior orbit portal in approaching the prechiasmatic target location. One nasal portal and a contralateral medial orbit portal created an angle between instruments of 28.3 degrees, essentially the same (28.6 degrees) as the angle using bilateral medial orbit portals. Distances to targets for the prechiasmatic location ranged from 60.0 mm for the medial orbit portal to 93.2 mm for the nasal portal, which is a reduction of 36.0%. An incrementally lower percentage reduction was observed as the target was located more posterior and inferior. Reduction percentages in length from nasal to medial orbit portals for the postchiasmatic, third ventricle, basal

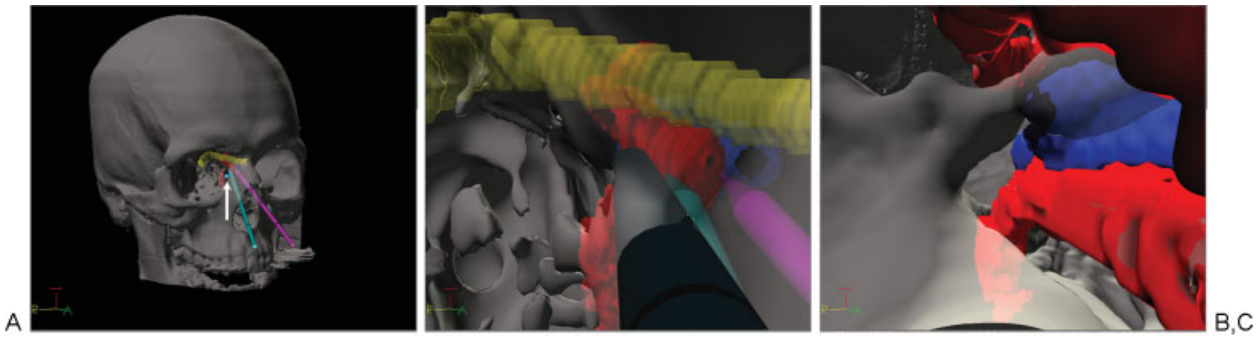

Fig. 5 Virtual endoscopy through a right medial orbit portal (arrow) to visualize the left cavernous sinus (blue). The optic nerve and chiasm (yellow) and the left internal carotid artery (red) are also seen. Two transnasal approach vectors and a right medial orbit portal (arrow; **a**). The view midway down the path of the right medial orbit portal; the instrument tips from the bilateral nasal portals are seen (**b**). The view of the left cavernous sinus behind the left internal carotid artery (**c**).

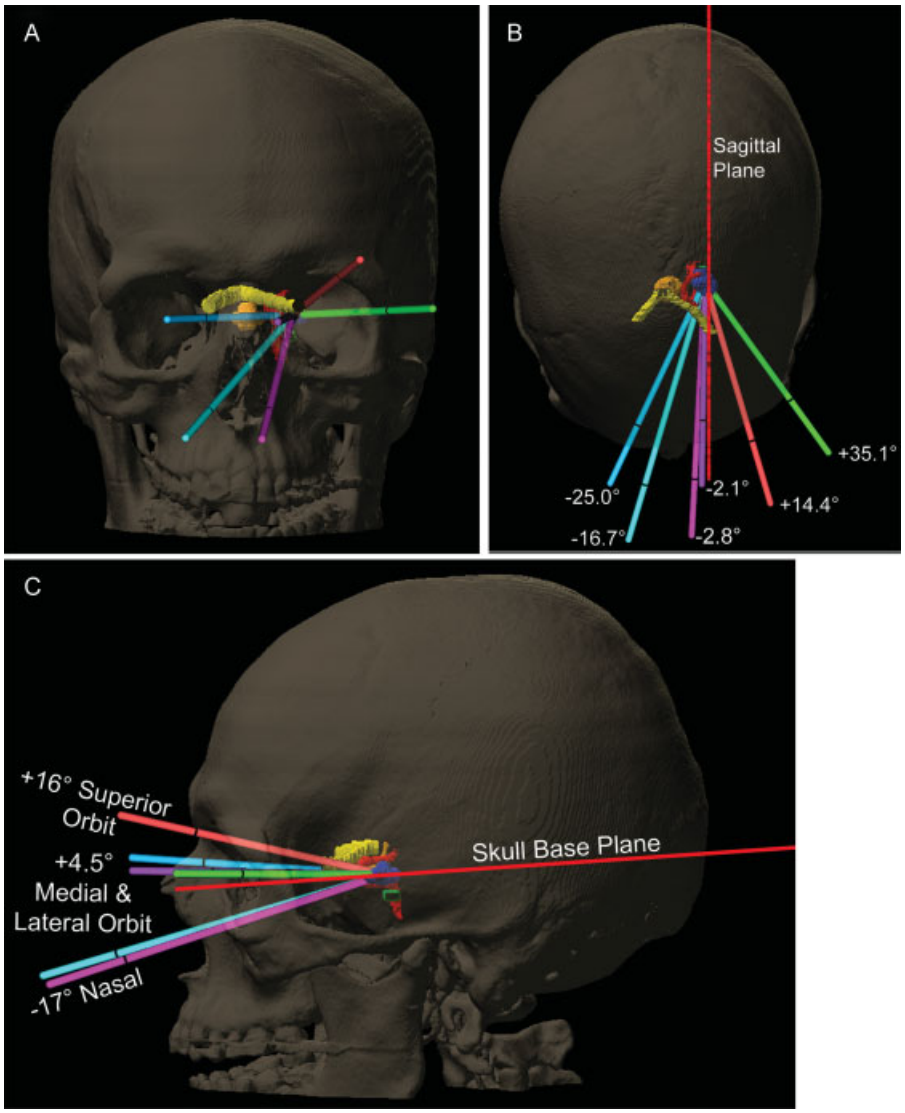

Fig. 7 Approach vectors using portals created by entry points of right and left medial orbit, right and left nasal, left superior orbit, and left lateral orbit: coronal view (**a**), axial view with average angle values with respect to a midsagittal plane (**b**), and sagittal view with average angle values with respect to a skull base plane (**c**).

cistern, and clivus target locations were 32.2%, 32.0%, 26.8%, and 20.9%, respectively.

The surgical approaches were performed on cadaver specimens for each target location. A direct comparison of the predicted angle from the model versus the physical measurements was done. These values were highly correlated (R^2 value: 0.91 for the angles and R^2 value: 0.97 for the distances) and are displayed in scatterplots, showing standard deviation and measurement error in ►**Figs. 8** and **9**. The vertical error bars in the scatterplot represent the measurement errors and resultant error propagation due to measuring a distance to report an angle (calculated using the law of cosines). The measured values were estimated to have a linear measurement error of 4 mm. Since distance measurements were used to calculate the angle between instruments, the error for the measured angles varies based on the acuity of the angle as a function of the law of cosines. The horizontal error bars are due to the estimated variance in reproducibly selecting an anatomical location on a CT scan; this was set to 2 mm.

Discussion

Although the idea of "minimally invasive" surgery is laudable, it is the nature of the pathology that dictates the invasiveness of a surgical approach. A realistic goal, however, is minimally disruptive surgery, and this is achieved by minimizing iatrogenic trauma. Surgical trauma can be minimized during two primary stages of the surgery; creation of the pathway to the target, and manipulation of the target. The use of computer modeling can aid in the performance of minimally disruptive surgery in both of these stages. With preoperative analysis, the shortest, most direct, and safest surgical pathways can be chosen, tested and practiced with virtual endoscopy; these can be combined as indicated in multiportal techniques. In the same manner, the angles of target visualization can be analyzed for adequacy, and the angles of surgical manipulation can be assessed to optimize the chances for a successful surgical outcome.

The choice of safe, effective surgical access to the skull base with minimal collateral tissue damage can be considered as a

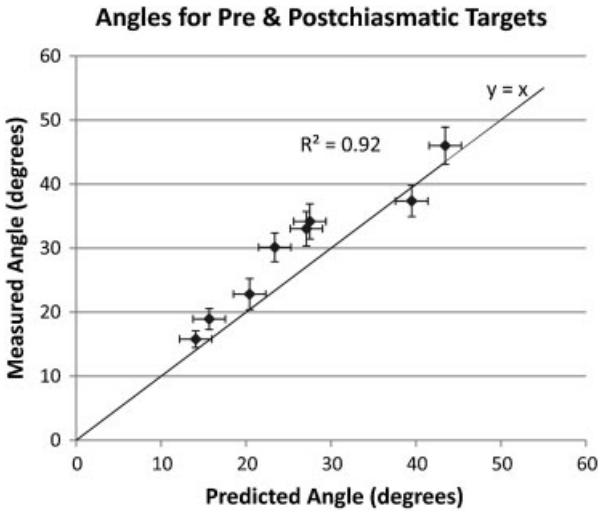

Fig. 8 Scatterplot of predicted angles derived from the computer model versus measured angles from the cadaver dissections. Results from bilateral nasal, nasal and opposite medial orbit, nasal and opposite superior orbit, and bilateral medial orbit are shown for two target locations.

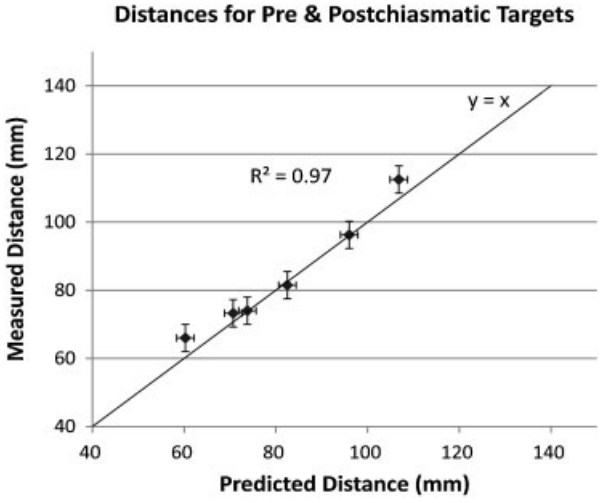

Fig. 9 Scatterplot of predicted distances derived from the computer model versus measured distances from the cadaver dissections. Results from nasal, medial orbit, and superior orbit portals are shown for two target locations.

complex geometric problem. There are many variables and constraints that include patient anatomy, possible surgical approaches, and target location within the skull base. The goal of this work was to create a model that includes the variables and constraints to find a solution that optimizes surgical access and visualization for given target locations.

The model created for this study provides a method to visualize and quantify approach combinations by calculating angles between instruments, approach angles with respect to anatomical planes, and length of approaches. The model was used to evaluate multiportal approach combinations for 11 specific locations in the sella and parasellar regions for 14 CT scans. The model was then tested on four cadaver specimens, and the calculations were found to be accurate and the approaches surgically feasible.

With the addition of transorbital to the available transnasal portals, the range of possible approach angles to a target increases substantially. A wide range of possible approach vectors offers the opportunity to choose portals that will optimize approach angles with respect to anatomical planes, but also to choose portals that will permit improved dissection capabilities. For certain lesions, it may be best to visualize or dissect perpendicular to a surface, and for others, to approach in a coplanar fashion. Expanded endonasal approaches have successfully accessed many of the targeted locations analyzed in this study, but the target manipulation capabilities through these approaches may not be optimal. When the tips of two instruments are working in coordination near the sella through transnasal approaches, the working depth is about 9 cm from the surface portal (the naris). The angle between the instruments in this situation is less than 15 degrees due to the lateral bone constraints at the pyriform aperture. This often results in hand or instrument tip collisions, especially when there are three or four instruments working simultaneously.

The angle between instruments that permits optimal dissection capabilities is a function of characteristics of the lesion and its location. A study that continuously recorded the orientation of instruments during open neurosurgical operations found a range of instrument angulation up to 73 degrees.[20] An endoscopic approach that minimizes collateral damage may not offer the full angulation of an open approach, but by choosing the appropriate portals it may be possible to recreate the angles needed for dissection in critical portions of the operation.

In addition to analyzing approach angles, it is also important to consider instrument range of motion and the size of the surgical portal. The majority of the transorbital portals analyzed in this study are modifications of existing approaches used to repair orbital fractures. Retraction of the orbital contents in the transorbital skull base approaches does not significantly increase the amount of displacement compared with the standard techniques used for orbital fracture repair. This amount of retraction permits the passage of common instruments needed, including a 4-mm endoscope (up to 6 mm with irrigation sheath), 2 to 3 mm suction device, fine dissection instruments (2 to 4 mm each), and a drill or ultrasonic bone aspirator (3 to 5 mm each). Prior cases published on transorbital neuroendoscopic surgery (TONES) routinely used 3 to 4 of the above instruments simultaneously through transorbital portals with adequate range of motion, and none of these cases resulted in loss of visual acuity or diplopia.[17,18]

A clinical application of this model is demonstrated in the following case: A 29-year-old female presented with visual field deficits, and on imaging was found to have a 1.5 cm cystic mass inferior and posterior to the optic chiasm (►**Fig. 10**). Computer planning analysis of bilateral nasal and medial orbit portals (►**Fig. 11**) demonstrated the following: the distance to the target location was 99.9 mm and 67.8 mm for the transnasal and medial orbit portals, respectively; the approach angle was 23.7 degrees (transnasal) and 8.1 degrees (medial orbit) to the skull base plane; the possible angles between portals were 13.7 to 28.7 degrees (►**Table 3**). Of

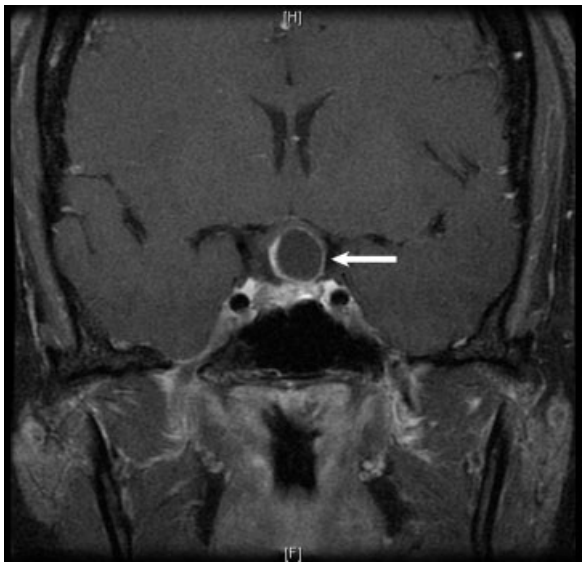

Fig. 10 Coronal T1 image showing a 1.5 cm postchiasmatic cystic mass (arrow).

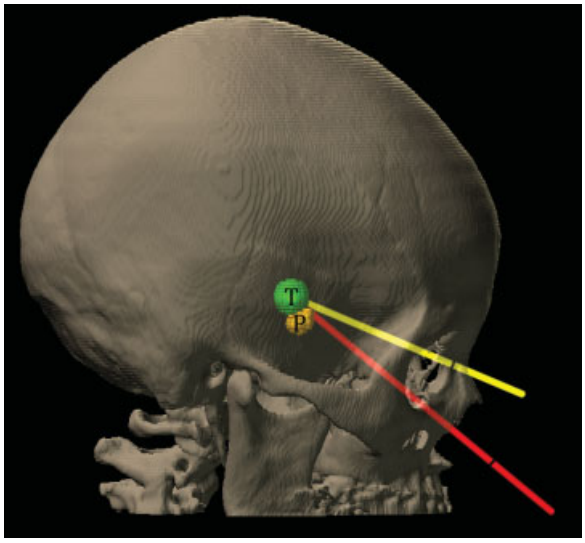

Fig. 11 Computer planning sagittal view showing approach vectors for nasal (red) and medial orbit (yellow) portals. The mass volume is defined (green, labeled T) posterior and superior to the pituitary gland (orange, labeled P).

note, the entrance location for the orbit portal is approximated by the medial canthus; this represents the smallest angle possible when approaching a near-midline target, whereas the transnasal portal entrance location is placed as laterally (largest angle) as possible as constrained by the pyriform aperture for a near-midline target.

Table 3 Angle between surgical approach portals to approach lesion seen in ►**Figs. 10** and **11**

Portal combinations	Angle between portals (degrees)
Bilateral nasal	13.7
Nasal and opposite medial orbit	26.3
Bilateral medial orbit	28.7

The modeling and visualization suggest that incorporating a medial orbit portal in this case will decrease the distance to the target by 32 mm (32%), double the angle between instruments, and approach from a vector 15.6 degrees superior compared with transnasal portals alone. An approach from a more superior vector may provide benefit in visualization, but also may require less manipulation and retraction of the pituitary gland. This approach would be nearly coplanar with the optic nerves and chiasm, potentially offering injury protection during mass excision.

This work represents a pilot study in the use of computer modeling to design and optimize surgical approaches to the skull base. This study is limited in that a relatively small number of targets in a localized region of the skull base were analyzed; however, the same methodology can be applied for all areas of the skull base. Similarly, the analysis of surgical portals was limited to two transnasal and eight transorbital pathways. This was necessary due to the exponentially increasing number of possible solutions with each added surgical portal and target location. Further advancements in the current labor-intensive process of choosing point locations, exporting, and processing data will make it possible to simultaneously analyze many more locations and surgical portals. Additional improvements to the model will include incorporating curved instruments, angled endoscopes, and haptic feedback to the user, offering information on tumor consistency.

An exciting future challenge will be to create an algorithm that searches for new portals and ideal portal combinations based on variables and constraints that can be inputted to account for the patient's individual anatomy and lesion location. Such programs currently exist for cardiothoracic and urologic surgery that help the surgeon optimally place the instrument and endoscope portals on the chest wall and abdomen.[21,22] Future efforts will determine ideal working angles between instruments and the number of portals needed to perform specific surgical tasks. A simulated environment could be created based on anatomical constraints at the target site and the constraints from the instrument portals to test the ability to perform surgical tasks at various approach angles and distances from the target. This data would be valuable to incorporate into the analysis.

The model and the quantitative data describing the surgical approaches provide an opportunity to assess robotic surgical platforms on the skull base, which has had limited clinical success to date. This is mainly due to the large size of available robotic systems and their instruments, and the narrow funnel effect encountered when operating through binarial portals. Despite this, access to certain regions has been demonstrated using transoral, transcervical, and transmaxillary approaches to widen the angle between instruments.[23–26] The angles computed in this study combining transnasal and transorbital portals were around 30 degrees or greater, compared with less than 15 degrees for binarial portals. This increased angulation may prove adequate to accommodate two or more robotic arms, even with the relatively large size of current robotic systems.

Conclusions

A computer model was created to analyze and optimize combinations of transorbital and transnasal portals to surgically access 11 specific locations in the sellar and parasellar regions. The distances and approach angles for each pathway were computed. The model suggested that the use of the transorbital portals can significantly decrease the length to the target while widening the potential angle between instruments. These findings were tested and validated on four cadaver specimens, with confirmation of the model results. Although the model was applied exclusively to the sella and parasellar region for this report, the methodology can be applied to any location in the skull base and brain.

The results of this study suggest that computer modeling holds the potential to play an integral role in the design, analysis, and testing of new surgical approaches, as well as in the selection of optimal approach strategy for the unique pathology of an individual patient.

Acknowledgments

The work of the entire University of Washington Institute for Simulation and Interprofessional Studies staff is much appreciated, especially that of Jonathan Del Toro-Chacon, Samuel Park, Megan Sherman, and Farrah Leland. We appreciate the consultation advice from the University of Washington Department of Statistics, Paul Sampson, PhD, and Yuan Chiam. Special thanks to Maria Cudejkova, RN. Stryker Corporation provided access to the iNtellect Cranial Navigation program. R.A.B. was supported by NIH T32 DC00018 and by the University of Washington Department of Otolaryngology-Head and Neck Surgery Resident Research Fund.

References

1 Kassam AB, Prevedello DM, Carrau RL, et al. The front door to meckel's cave: an anteromedial corridor via expanded endoscopic endonasal approach- technical considerations and clinical series. Neurosurgery 2009;64(3, Suppl):ons71–ons82, discussion ons82–ons83
2 Zada G, Du R, Laws ER Jr. Defining the "edge of the envelope": patient selection in treating complex sellar-based neoplasms via transsphenoidal versus open craniotomy. J Neurosurg 2011;114: 286–300
3 Romano A, Chibbaro S, Marsella M, et al. Combined endoscopic transsphenoidal-transventricular approach for resection of a giant pituitary macroadenoma. World Neurosurg 2010;74: 161–164
4 Alleyne CH Jr, Barrow DL, Oyesiku NM. Combined transsphenoidal and pterional craniotomy approach to giant pituitary tumors. Surg Neurol 2002;57:380–390, discussion 390
5 Greenfield JP, Leng LZ, Chaudhry U, et al. Combined simultaneous endoscopic transsphenoidal and endoscopic transventricular resection of a giant pituitary macroadenoma. Minim Invasive Neurosurg 2008;51:306–309
6 Ojha BK, Husain M, Rastogi M, Chandra A, Chugh A, Husain N. Combined trans-sphenoidal and simultaneous trans-ventricular-endoscopic decompression of a giant pituitary adenoma: case report. Acta Neurochir (Wien) 2009;151:843–847, discussion 847
7 de Notaris M, Prats-Galino A, Cavallo LM, et al. Preliminary experience with a new three-dimensional computer-based model for the study and the analysis of skull base approaches. Childs Nerv Syst 2010;26:621–626
8 de Notaris M, Solari D, Cavallo LM, et al. The use of a three-dimensional novel computer-based model for analysis of the endonasal endoscopic approach to the midline skull base. World Neurosurg 2011;75:106–113, discussion 36–40
9 Bernardo A, Preul MC, Zabramski JM, Spetzler RF. A three-dimensional interactive virtual dissection model to simulate transpetrous surgical avenues. Neurosurgery 2003;52:499–505, discussion 504–505
10 Kakizawa Y, Hongo K, Rhoton AL Jr. Construction of a three-dimensional interactive model of the skull base and cranial nerves. Neurosurgery 2007;60:901–910, discussion 901–910
11 Tolsdorff B, Pommert A, Höhne KH, et al. Virtual reality: a new paranasal sinus surgery simulator. Laryngoscope 2010;120:420–426
12 Prosser JD, Figueroa R, Carrau RI, Ong YK, Solares CA. Quantitative analysis of endoscopic endonasal approaches to the infratemporal fossa. Laryngoscope 2011;121:1601–1605
13 Qiu TM, Zhang Y, Wu JS, et al. Virtual reality presurgical planning for cerebral gliomas adjacent to motor pathways in an integrated 3-D stereoscopic visualization of structural MRI and DTI tractography. Acta Neurochir (Wien) 2010;152:1847–1857
14 Filipce V, Pillai P, Makiese O, Zarzour H, Pigott M, Ammirati M. Quantitative and qualitative analysis of the working area obtained by endoscope and microscope in various approaches to the anterior communicating artery complex using computed tomography-based frameless stereotaxy: a cadaver study. Neurosurgery 2009;65:1147–1152, discussion 1152–1153
15 Beretta F, Andaluz N, Chalaala C, Bernucci C, Salud L, Zuccarello M. Image-guided anatomical and morphometric study of supraorbital and transorbital minicraniotomies to the sellar and perisellar regions: comparison with standard techniques. J Neurosurg 2010;113:975–981
16 Cavalcanti DD, García-González U, Agrawal A, et al. Quantitative anatomic study of the transciliary supraorbital approach: benefits of additional orbital osteotomy? Neurosurgery 2010;66(6, Suppl Operative):205–210
17 Moe KS, Bergeron CM, Ellenbogen RG. Transorbital neuroendoscopic surgery. Neurosurgery 2010;67(3, Suppl Operative): ONS16–ONS28
18 Balakrishnan K, Moe KS. Applications and outcomes of orbital and transorbital endoscopic surgery. Otolaryngol Head Neck Surg 2011;144:815–820
19 Ciporen JN, Moe KS, Ramanathan D, et al. Multiportal endoscopic approaches to the central skull base: a cadaveric study. World Neurosurg 2010;73:705–712
20 Woerdeman PA, Willems PW, Noordmans HJ, van der Sprenkel JW. The analysis of intraoperative neurosurgical instrument movement using a navigation log-file. Int J Med Robot 2006;2:139–145
21 Ogata M, Nagasaka M, Inuiya T, Makiyama K, Kubota Y. A development of surgical simulator for training of operative skills using patient-specific data. Stud Health Technol Inform 2011;163:415–421
22 Bauernschmitt R, Feuerstein M, Traub J, Schirmbeck EU, Klinker G, Lange R. Optimal port placement and enhanced guidance in robotically assisted cardiac surgery. Surg Endosc 2007;21:684–687
23 McCool RR, Warren FM, Wiggins RH III, Hunt JP. Robotic surgery of the infratemporal fossa utilizing novel suprahyoid port. Laryngoscope 2010;120:1738–1743
24 O'Malley BW Jr, Weinstein GS. Robotic anterior and midline skull base surgery: preclinical investigations. Int J Radiat Oncol Biol Phys 2007;69(2, Suppl):S125–S128
25 Lee JY, O'Malley BW Jr, Newman JG, et al. Transoral robotic surgery of the skull base: a cadaver and feasibility study. ORL J Otorhinolaryngol Relat Spec 2010;72:181–187
26 Kupferman M, Demonte F, Holsinger FC, Hanna E. Transantral robotic access to the pituitary gland. Otolaryngol Head Neck Surg 2009;141:413–415